

Spin states and phase separation in $\text{La}_{1-x}\text{Sr}_x\text{CoO}_3$
 ($x = 0.15; 0.25; 0.35$) in s: optical, magneto-optical and
 magneto-transport studies

N. N. Loshkareva,¹ E. A. Gan'shina,² B. I. Bevtsev,³ Yu. P. Sukhonukov,¹ E. V. Mostovshchikova,¹ A. N. Vinogradov,² V. B. Krasovitsky,³ and I. N. Chukanova⁴

¹Institute of Metal Physics of Ural Division of RAS, Ekaterinburg, 620219, Russia

²Moscow State University, Moscow, 119899, Russia

³B. Verkin Institute for Low Temperature Physics and Engineering,
 National Academy of Sciences, Kharkov 61103, Ukraine

⁴Institute for Single Crystals, National Academy of Sciences, Kharkov 61001, Ukraine

Abstract

Optical absorption and transverse Kerr effect spectra, resistivity and magnetoresistance of $\text{La}_{1-x}\text{Sr}_x\text{CoO}_3$ ($x = 0.15; 0.25; 0.35$) in s have been studied. The temperature dependencies of the optical and magneto-optical properties of the in s exhibit features, which can be attributed to the transition of the Co^{3+} ions from the low-spin state ($S = 0$) to the intermediate-spin state ($S = 1$) and to orbital ordering of the Co^{3+} ions in the latter state. The evolution of the properties influenced by doping with Sr is interpreted on the basis of the phase separation model.

PACS numbers: 72.80.Ga; 78.66.-w; 78.20.Ls

bevtsev@ilt.kharkov.ua

I. INTRODUCTION

The discovery of the so-called colossal magnetoresistance in manganite LaMnO_3 [1] has renewed an interest in other ferromagnetic perovskite-like compounds. These include LaCoO_3 -based cobaltites which are in many ways similar to manganites and yet they have some fundamental distinctions. At low temperatures, LaCoO_3 is a non-magnetic insulator. In this state Co^{3+} ions are mainly in the low-spin (LS) state ($t_{2g}^6; S = 0$) [2] because the crystal field energy dominates slightly over the intraatomic Hund's energy [2, 3]. However, as the temperature rises, Co^{3+} ion state changes gradually from the LS state to the high-spin (HS) state ($t_{2g}^4 e_g^2; S = 2$) or to the intermediate-spin (IS) state ($t_{2g}^5 e_g^1; S = 1$). The latter scenario is supported by the theoretical calculations [3, 4] and results of some experimental studies [5, 6, 7, 8]. The problem of spin states of Co^{3+} ions in cobaltites is not settled to date and remains topical.

When LaCoO_3 is doped with Sr^{2+} ions, hole-rich regions appear in the hole-poor matrix [9]. Evolution of the magnetic properties as a function of Sr^{2+} concentration x and temperature is governed by the transition from the spin-glass-like to cluster-glass state or to the ferromagnetic (FM) metallic state [10, 11]. The certain scatter in the estimates obtained by different authors [9, 10, 11] for the critical Sr^{2+} concentration at which long-range FM order sets in is accounted for by such factors as instability against the formation of clusters rich in Sr^{2+} and containing ions in the IS state, the dependence of the chemical heterogeneity upon the thermal history of the samples and the degree of oxidation. The question is still discussed considerably whether clusters are generated by compositional inhomogeneities when, for example, the phases with $x = 0.5$ and $x = 0.2$ are present in $\text{La}_{0.85}\text{Sr}_{0.15}\text{CoO}_3$ [12] or they appear due to electron phase separation [13].

In this article, a study of the Kerr effect, optical absorption and transport phenomena in $\text{La}_{1-x}\text{Sr}_x\text{CoO}_3$ ($x = 0.15; 0.25; 0.35$) LaMnO_3 is presented. The phase separation in LaMnO_3 can be expected to be somewhat more complicated as compared with bulk materials since it could depend on strain induced by the La -substrate lattice mismatch. At the same time,

LaMnO_3 are suitable objects which can be investigated by traditional electric and magnetic techniques giving averaged characteristics of the (inhomogeneous) material and by optical methods permitting to separate responses from conducting regions and the insulating matrix and to study the magnetic processes inside the conducting clusters. This combined approach was applied earlier to manganites [14, 15]: the charge inhomogeneities were studied by the optical absorption technique while the magnetically inhomogeneous state was investigated using magneto-optical (MO) method.

Transport and optical properties of FM oxides are known to depend significantly on their magnetic properties. As for the MO properties, they are determined directly by the magnetization of a material studied. In this work, the MO properties were measured using the transverse Kerr effect (TKE). Generally, the MO Kerr effect consists in an influence of the magnetization of the medium on the reflected light. The TKE consists in the intensity variation of a light reflected by a magnetized sample in conditions where magnetic field is applied parallel to the sample surface and perpendicular to the light incidence plane. Measurements of MO spectra in the visible and near ultra-violet spectral range, i.e. in the range of the fundamental absorption, could provide an information concerning electronic structure of the cobaltites and its dependence on chemical composition, conditions of the synthesis and other factors. In particular, the appearance of the new type of magnetic ions, Co^{4+} , due to doping with Sr, and/or change in the spin state of Co ions are expected to

influence the MO spectra. The magnitude of the MO response is known to be the product of spin-orbit coupling strength and net electron spin polarization (magnetization). This makes the magneto-optical effects sensitive to the magnetic state of unfilled d-shells in the transition-metal ions. MO spectroscopy provides not only the information about the total density of states (similarly to normal optical measurements) but also about the electron spin polarization of states participating in the magneto-optical transition [16, 17].

The temperature dependence for different MO effects measured at a definite wavelength indicates the variation of the magnetic order in the samples. Temperature and magnetic field dependences of MO effects reveal the phase transition temperatures and peculiarities of the originated magnetically ordered states. MO response is sensitive not only to the long-range magnetic order but even to the short-range magnetic order. Thus, formation of the ferromagnetic clusters would manifest itself in the MO properties.

The phenomenological description of MO effects is based on consideration of the influence of a magnetic field on the dielectric permittivity tensor, ϵ_{ij} , of the medium [17]. If the tensor is symmetric ($\epsilon_{ij} = \epsilon_{ji}$) in zero magnetic field $H = 0$, it becomes non-symmetric [$\epsilon_{ij}(H) = \epsilon_{ji}(-H)$] in a nonzero magnetic field. In the linear approximation, the dielectric permittivity tensor of the gyroelectric medium is

$$\epsilon = \begin{pmatrix} \epsilon_0 & i\epsilon_{xy} & 0 \\ -i\epsilon_{xy} & \epsilon_0 & 0 \\ 0 & 0 & \epsilon_0 \end{pmatrix}; \quad (1)$$

where the diagonal elements, $\epsilon_0 = \epsilon_0^0 - i\epsilon_0^{\text{im}}$, describe normal optical properties (which do not depend on magnetization) and off-diagonal elements, $\epsilon_{xy} = \epsilon_{xy}^0 - i\epsilon_{xy}^{\text{im}}$, proportional to magnetization, are related to MO properties. All MO effects, which are linear in magnetization, can be expressed in terms of off-diagonal elements of the dielectric permittivity tensor.

For the TKE, variation of the reflected light intensity for p-polarized wave due to the magnetization of a ferromagnetic sample can be written as [17]

$$I_p = 2 \sin(2') \frac{A_1}{A_1^2 + B_1^2} \epsilon_{xy}^0 + 2 \sin(2') \frac{B_1}{A_1^2 + B_1^2} \epsilon_{xy}^{\text{im}}; \quad (2)$$

where $A_1 = \epsilon_0^0 [2\epsilon_0^0 \cos^2(\theta') - 1]$, $B_1 = [\epsilon_0^{\text{im}2} - \epsilon_0^0] \cos^2(\theta') + \epsilon_0^0 \sin^2(\theta')$, θ' is incidence angle of light.

The results presented in this article can be taken as supporting the transition of the Co^{3+} spins from the LS to the IS state with increasing temperature. Beside this, the results agree with the presence of the orbital ordering of the Co^{3+} ions in the IS state. At consideration of changes in the properties of the films with Sr doping the phase-separation effect is taken into account.

II. SAMPLES AND EXPERIMENTAL TECHNIQUES

The films (about 200 nm thick) were grown by pulsed-laser deposition onto a (001)-oriented LaAlO_3 substrate with a 1.06 μm Nd-YAG laser (pulse length 10 ns, pulse energy 0.33 J, pulse frequency 12 Hz). The ceramic targets with nominal compositions $\text{La}_{1-x}\text{Sr}_x\text{CoO}_3$ ($x = 0.15; 0.25; 0.35$) were prepared by solid-state reaction method. We were aware that available methods of chemical control can determine actual compositions in targets and films with an accuracy not better than ± 2 atomic percent. Besides, the composition

of pulsed-laser deposited films can differ slightly from that of the target. For all these reasons, the nominal compositions were chosen in such way that one of them ($x = 0.15$) is sure below the percolation threshold ($x_c = 0.20\{0.25$) [9, 10, 11], at which the infinite FM cluster is formed below the Curie temperature in this system, the second ($x = 0.25$) should be near the percolation threshold, and the third ($x = 0.35$) is sure above this threshold. The results outlined in the following sections show that we have achieved this aim to a great extent.

At the ablation of target material, the substrate was shielded to avoid its direct exposure to the plasma plume. In this case the deposition occurs from the flux that is reflected from a side screen. This has ensured a high surface smoothness, which is essential for obtaining reliable results at an optical study. The deposition was performed in oxygen atmosphere at the pressure 8 Pa and the substrate temperature 880–950 °C. The deposited films were cooled to room temperature in oxygen at 10^5 Pa (1 atm). These preparation conditions make possible coherent epitaxy. The investigations of other cobaltite films, prepared in the same pulsed-laser deposition chamber and in the same conditions, provide reason enough to suggest that the films studied are polycrystalline, even if rather highly oriented.

The optical absorption spectra of the films were measured at 80–295 K with a prism infrared spectrometer (in the range 0.1–1.4 eV) and a grating spectrometer (in the range 1.0–4.0 eV). The measurements of TKE were made using an automatic MO spectrometer [18]. A dynamic method to record TKE was used. The relative change in the intensity of the reflected light $\Delta I = [I(H) - I(0)]/I(0)$, where $I(H)$ and $I(0)$ are the intensities of the reflected light in the presence and in absence of a magnetic field respectively, was directly measured in the experiment. The magnitude of the alternating magnetic field in the gap of an electromagnet was up to 3.5 kOe. The relative precision of the apparatus is 10^{-5} . MO spectra were recorded in the photon energy range 1.3–3.8 eV at a fixed light incidence angle $\theta = 67^\circ$. For MO measurements, a continuous-flow helium cryostat is used, which makes possible investigations in the temperature range 10–300 K.

The resistivity of the films was measured as a function of temperature and magnetic field (up to 20 kOe) using the standard four-point probe technique. The field was applied parallel or perpendicular to the film plane. In both cases it was perpendicular to the transport current.

III. EXPERIMENTAL RESULTS

A. Kerr effect

The temperature dependences of TKE measured on $\text{La}_{1-x}\text{Sr}_x\text{CoO}_3$ films (in the magnetic field $H = 3.5$ kOe and at photon energy $E = 2.8$ eV) are shown in Fig. 1. The $\Delta I(T)$ curves reveal characteristic features at the transition to the magnetically ordered state. The position of the abrupt decrease in TKE on the temperature scale (when going from lower to high temperature) corresponds to the Curie temperature T_c . As follows from given curves, Curie temperatures for films with $x = 0.35$ and $x = 0.25$ coincide and are equal to 230 K. Below 230 K the film with $x = 0.25$ exhibits a considerable magneto-optical effect with a peak at $T = 180$ K. As temperature decreases further, TKE drops sharply: its value becomes more than three times smaller in the range 110–160 K for $x = 0.35$ or in the range 130–175 K for $x = 0.25$. For the film with $x = 0.15$, TKE has a peak at $T = 118$ K and another anomaly at $T = 60$ K. Note that in the low temperature region ($T < 118$ K), TKE for $x = 0.15$ is larger than for films with higher Sr concentrations. The $\Delta I(T)$ shape is dependent

considerably on measurement conditions. As seen in Fig. 1, the TKE curves for $x = 0.15$ and $x = 0.35$ measured on cooling and heating in a high field ($H = 3.5$ kOe) are shifted relative to each other. Hysteresis phenomena were much smaller for the Im with $x = 0.25$ and were observed only near the maximum.

The position of the maximum in the TKE temperature curve is dependent on the applied magnetic field and shifted to the high-temperature region when the field decreased. On heating the Im with $x = 0.35$ in the field $H = 0.9$ kOe, the (T) curve shifts drastically (over 70 K) towards higher temperatures [Fig. 1(c)] when compared with the (T) curve taken in the higher field $H = 3.5$ kOe. Both the curves nearly coincide at $T > 200$ K. On a fast cooling (with a rate about 20 K/min) of the Im with $x = 0.25$, the (T) curve shifts to the high-temperature region enormously and the maximum magnitude of TKE decreases greatly [Fig. 1(b)]. At $T < 110$ K, TKE for Im s with $x = 0.25$ decreases linearly with temperature (Fig. 1).

The spectral dependences of TKE measured at temperatures of the maximum in their temperature curves are shown in Fig. 2. It is seen that the spectra are similar for all Sr concentrations studied. The Kerr effect has a positive maximum at $E = 1.5$ eV and a broad negative maximum in the range of $E = 2.7$ eV. The amplitudes of the peaks increase with the growing Sr concentration. Above 2.0 eV the spectra exhibit a fine structure which is most distinct for the Im with $x = 0.15$ (peculiar features at 2.1, 2.6 and 3.1 eV stand out against the background of the broad maximum).

The field dependences of TKE, (H) , for low-temperature range are linear for all Im s studied (Fig. 3). They are, however, quite different near the temperatures corresponding to maximum in (T) dependences. For the Im with $x = 0.15$ the (H) is linear up to 3.5 kOe, whereas for Im s with $x = 0.25$ and $x = 0.35$ it looks like a field-magnetization curve for FM compounds.

B. Resistivity and magnetoresistance

The temperature dependences of resistivity, (T) , for the Im s studied are presented in Fig. 4 in semilogarithmic coordinates. Since resistivity of the Im with $x = 0.35$ shows only small visible temperature variation in this scale, it is presented more clearly in Fig. 5 in linear coordinates. Dependences (T) for Im s with $x = 0.15$ and $x = 0.25$ have non-metallic character ($d\rho/dT < 0$) (Fig. 4). They are found to be rather unusual: (T) follows closely the dependence $(T) = (0) \exp(-\alpha T)$ for $x = 0.15$ and is practically linear in temperature for $x = 0.25$. The dependence (T) for $x = 0.35$ has a maximum at $T = 250$ K and a shallow minimum at $T = 40$ K (Fig. 5). The minimum is most probably connected with a polycrystalline structure of the Im [19]. The behavior of (T) is metallic between these extremum points.

The temperature dependences of magnetoresistance $(MR) \quad R(H) - R(0) = \Delta R(H) = R(H) - R(0)$ measured in the magnetic field $H = 20$ kOe are shown in Fig. 6. It is seen that for this field the MR is negative for all Im s studied. The dependence taken on the sample with $x = 0.35$ is quite typical of optimally doped FM cobaltites and manganites [Fig. 6(a)]: there is a quite pronounced peak (in the MR modulus) near the Curie temperature $T_c = 230$ K; it goes down for temperature deviating to either side from T_c . This type of MR behavior is characteristic of so called intrinsic mechanism of MR, which depends on the magnetic order (an external field enhances the magnetic order that, in its turn, leads to a decrease in the resistivity and, therefore, to negative MR). This mechanism works in the

FM state only. For this reason the MR decreases to zero for temperatures above T_c . Far below T_c , the MR of this type goes to zero as well since an applied magnetic field can not strengthen the magnetic order appreciably in low temperature range ($T \ll T_c$) where the magnetization is close to saturation.

In a magnetically inhomogeneous sample, consisting of weakly connected FM regions in dielectric or non-magnetic matrix, the so called extrinsic mechanisms of MR can give an additional contribution to the total MR. These mechanisms are determined by the charge transfer between the poorly connected or isolated FM regions. This type of magnetic inhomogeneity in FM oxides can be connected with grain boundaries in polycrystalline samples or with the phase separation effects. A contribution of the extrinsic MR increases with temperature decreasing and is maximum at zero temperature. A concurrence of the intrinsic and extrinsic MRs can result in non-monotonic temperature dependence of the total measured MR in cobaltite films [19, 20]. Discussion of possible mechanisms for the extrinsic type of MR in inhomogeneous polycrystalline samples can be found in Refs. [21]. It is clear that these mechanisms are applicable (at least generally) also in the case of the phase separation when this results in a system of hole-rich FM clusters embedded in hole-poor dielectric matrix. In this way, the temperature behavior of MR in FM oxides can reflect their magnetic homogeneity. Taking it all into account, it can be said from Fig. 6(a) that film with $x = 0.35$ is the most homogeneous from the films studied although even it has appreciable MR at low temperature range that indicate the presence of some magnetic inhomogeneity induced by one or both of the above-mentioned reasons. The MR of the film with $x = 0.25$ increases continuously with temperature decreasing [Fig. 6(b)] what corresponds to behavior of highly inhomogeneous system. The same is true in relation to the film with $x = 0.15$ where additionally a non-monotonic temperature behavior of MR can be seen. It should be noted that the largest MR is observed in the least doped sample ($x = 0.15$) [Fig. 6(c)]. For the film with $x = 0.15$ and 0.25 , the temperature interval, where MR increases with lowering temperature, is fairly close to the temperature range of increasing TKE.

The MR of the film with $x = 0.35$ and $x = 0.15$ is anisotropic (Fig. 6). The absolute values of negative MR are much higher in fields parallel to the film plane than in perpendicular ones. The anisotropic MR is not surprising for pulsed-laser deposited films of FM perovskite oxides. For cobaltites, this effect is seen earlier in $\text{La}_{0.5}\text{Sr}_{0.5}\text{CoO}_3$ film [19]. Since the conductivity in mixed-valence cobaltites increases with an enhancement of the FM order, this behavior just reflects the point that the magnetization increases more easily in a magnetic field parallel to the film plane. It is connected mainly with the shape anisotropy of the magnetization. The strain-induced anisotropy due to the film-substrate lattice interaction can have an influence as well. The influence of this type of MR anisotropy has been found in $\text{La}_{0.5}\text{Sr}_{0.5}\text{CoO}_3$ film [20]. All these types of the MR anisotropy are associated with FM state and, for this reason, disappear above T_c . In the films studied, MR anisotropy is found only below $T = 200$ K for $x = 0.15$ and below $T = 250$ K for $x = 0.35$. The highest MR anisotropy is observed in the film with $x = 0.15$ [Fig. 6(c)]. No appreciable MR anisotropy is found in the film with $x = 0.25$.

Generally, the MR curves of the films studied have been hysteretic with specific structures in low fields (see Fig. 7 for $x = 0.35$ at $T = 78$ K). It is well established that the behavior of the MR curves for FM oxides correlates with that of magnetization curves [21]. In particular, the field $H = H_p$, where the resistance reaches its maximum (Fig. 7), corresponds to the coercive force H_c . It is found that field H_p is maximal at lowest temperature in this study ($T = 4.2$ K) but it drops to zero above $T = 77$ K for $x = 0.15$ and above $T = 90$ K

for $x = 0.35$. Above certain field values, hysteresis no longer occurs, which implies that magnetization reversal processes start in these fields. Such fields are much lower for the parallel orientation (Fig. 7). We will discuss the hysteresis phenomena more elaborately below.

C. Optical absorption

The optical density spectra $D = \ln(I_0/I) = \ln(1/t)$ (I_0 is the incident-light intensity, I is the intensity of light transmitted through the film, t is the transmittance) in the visible and infrared (IR) ranges are shown in Figs. 8 and 9, respectively. The optical density spectrum (corresponds to absorption spectrum where the reflection and film thickness was not taken into account) for the film with $x = 0.15$ has a wide band at $E = 3.0$ eV and quite narrow bands at about 1.15, 1.9, 2.4 eV in the fundamental absorption region (Fig. 8). When the Sr concentration is increased, the low-energy band (1.15–0.03) eV shifts slightly towards higher energies. For $x = 0.35$ it is centered at 1.3 eV. The 1.9 eV band broadens and shifts towards lower energies.

For the film with $x = 0.15$, absorption in the IR range goes up for energy increasing above 0.9 eV (Fig. 9), which indicates the onset of fundamental absorption. At $E < 0.9$ eV the light interaction with charge carriers contributes to the absorption of the film with $x = 0.25$ and $x = 0.35$. As follows from the reflection spectra for LaCoO_3 [22], phonon absorption begins below 0.08 eV.

The absorption in the film with $x = 0.15$ is considerably lower at 80 K than at 295 K in the IR range (Fig. 9). For the film with $x = 0.25$ the absorption in the region $E < 0.9$ eV is slightly higher at 80 K than at 295 K. For the film with $x = 0.35$ the absorption at $E < 0.9$ eV is considerably higher at 80 K than at room temperature, which implies that the contribution of charge carriers to the spectrum is larger for $x = 0.35$ than for $x = 0.25$.

As shown for manganites [14, 15, 23], in the energy range of light interaction with charge carriers, the behavior of $t(T)$ [or transmitted light intensity $I(T)$] follows the temperature behavior of resistivity in the case that metallic FM region percolates through the whole material. For the manganites, which for some reasons consist of separated metallic regions embedded in semiconducting matrix, the $I(T)$ dependence reflects the temperature behavior of the resistivity in these isolated metallic regions (or clusters) and this behavior can be quite different from the direct-current $\rho(T)$ dependences. The $I(T)$ behavior in Sr-doped cobaltite films at $E = 0.20$ eV is shown in Fig. 10(a). On cooling the transmitted light intensity (transmittance) of the film with $x = 0.15$ increases, i.e. the transmittance behavior is semiconductive at 80–300 K. In the film with $x = 0.25$ the transmittance exhibits metallic temperature behavior at $T < 180$ K, although no this type of behavior can be seen in the $\rho(T)$ dependence (Fig. 4). In the film with $x = 0.35$ transmittance drops significantly below $T = 250$ K (metallic behavior), which is in agreement with the $\rho(T)$ behavior for this film (Fig. 5).

The $I(T)$ dependences of cobaltite films studied have an extra anomaly (most pronounced for $x = 0.35$) in the same temperature range 160–220 K (Fig. 10). This type of anomaly was never seen in manganites. The anomaly is observed not only at the photon energy range where light interaction with charge carriers occurs [Fig. 10(a)], but at the range of the fundamental absorption edge at $E = 1.0\{1.4$ eV [Fig. 10(b)] as well, where only small ($x = 0.25$, $x = 0.35$) or no ($x = 0.15$) contribution of charge carrier to absorption is expected. The anomaly is more complicated at $E = 1.0\{1.4$ eV [Fig. 10(b)] than at

$E = 0.20$ eV [Fig. 10(a)]. This may be connected with the intricate character of the spectrum near the fundamental absorption edge, where the closely spaced and spectrally unresolved absorption bands overlap. Note that in our experiments the spectral bandpass of slits in the two spectrometers used is different in the region of overlapping working ranges. The spectra in Fig. 8 measured with a smaller spectral bandpass are therefore resolved better than the spectra in Fig. 9.

The magneto-transmittance effect (analogous to magnetoresistance) detected in manganite films [24] is not found in cobaltite films studied up to $H = 10$ kOe apparently because cobaltites have much lower magnetoresistance. The influence of magnetic fields on transmittance of the films shows up itself, however, in rather different behavior of the $I(T)$ curves taken at $E = 0.20$ eV on cooling in zero and finite ($H = 8$ kOe) fields. The strong effect of the sample thermal magnetic prehistory is illustrated in Fig. 10(c). Curves 1-4 describe the $I(T)$ dependences under successive changes in measurement conditions. The $I(T)$ anomaly weakened on field cooling (FC) and measurement in $H = 0$ (curve 2) or on zero-field cooling (ZFC) and measurement in $H > 0$ (curve 3). The anomaly is suppressed completely when the film is heated above room temperature and then cooled quickly (curve 4). Additional explanatory comments to the measurement conditions can be found in caption to Fig. 10.

IV. DISCUSSION

A. Absorption spectra and Kerr effect

There are only scanty optical studies on $\text{La}_{1-x}\text{Sr}_x\text{CoO}_3$ [6, 22, 25, 26, 27]. It can be found among them optical conductivity spectra obtained by the Kramers-Kronig analysis of reflectivity spectra of poly- and single crystals [26]. The polar Kerr effect for $\text{La}_{1-x}\text{Sr}_x\text{CoO}_3$ single crystals at room temperature was studied in Ref. 27. The optical density spectra $D(E)$ of the films studied have more features in the visible range (Fig. 8) than the light conductivity spectra $\sigma(E)$ of $\text{La}_{1-x}\text{Sr}_x\text{CoO}_3$ single crystals with similar composition [26]. The $\sigma(E)$ spectra of single crystals have three bands at energies about 1, 3, and 6 eV, respectively [26]. They are attributed [28] to excitations into the e_g band from the t_{2g} band and broad O(2p) band split by the hybridization effects into the bonding and antibonding parts. The spectra of the cobaltite films studied have four bands in energy range 1.0-3.5 eV (Fig. 8). This can be presumably attributed to superposition of geometric resonances (surface plasmons) induced by structural inhomogeneities on charge transfer transitions (as shown for manganites in Ref. 29). Inhomogeneous structures may appear due to the phase separation, polycrystallinity of the films and strains at the film-substrate boundary. The evolution of absorption spectra with doping for the films studied is similar to that of single crystals [26]: as the Sr concentration increases, the spectral weight transfers from the visible range to the IR region, where light interaction with free charge carriers occurs.

The TKE magnitude is comparable in cobaltites (Fig. 2) and manganites [27]. The high value of the Kerr effect may be connected with the strong spin-orbit interaction expected for Co^{3+} (IS) ions. As for $\text{La}_{1-x}\text{Sr}_x\text{CoO}_3$ single crystal [27], TKE in the films studied was maximum in the broad band near 3.0 eV. In Ref. 27 this behavior was attributed to the d-d transition $t_{2g} \rightarrow e_g$ allowed for the majority-spin (or spin-up) states because of the hybridization with O(2p) orbitals. Large MO effect found in the films studied may also be related with this transition, which must take place only for Co^{3+} ions in the IS or HS states, but not in the LS state. Qualitatively, the TKE behavior can also be explained on the basis

of band calculation for LaCoO_3 with Co^{3+} (IS) ions [3]. According to the electron-energy scheme for Co ions in the IS state [3], the magneto-optical effect should first appear in the spin-up subband and reach its maximum at $E = 2.0$ eV. Then, at $E > 3.5$ eV the transitions in the spin-down subband can be expected. The competition of these transitions can also account for the change in sign and spectral behavior of the effect.

B. Temperature dependences of transmittance, Kerr effect, resistivity and magnetoresistance

It is found for lanthanum manganites of varying compositions [14, 15] that the temperature at which the FM contribution appears (estimated from the temperature dependences of TKE) agrees well with the temperature of the insulator-metal transition in the hole-rich separated regions or clusters (found from IR absorption data). A direct correlation of this type is not seen in cobaltite $\text{La}_x\text{Co}_{1-x}\text{O}_3$ studied [compare Figs. 1 and 10(a)]. We will try in the following to clear up a possible reason for this discrepancy. In doing so we can assume that the holes appearing with Sr doping of cobaltites cause phase separation into the hole-poor matrix and hole-rich regions (e.g., see [9, 10, 13]).

1. $\text{La}_{0.85}\text{Sr}_{0.15}\text{CoO}_3$ film

Our magneto-optical, optical, MR and MR anisotropy results for the film with $x = 0.15$ support the outlined general picture for magnetic processes in cobaltites with low doping level below the percolating threshold ($x_c = 0.20\{0.25\}$ [9, 10, 11]). The monotonic (except for the range 160{220 K) temperature dependence of intensity of the transmitted light at $E = 0.20$ eV in the film with $x = 0.15$ [Fig. 10(a)] suggests that the clusters with Co^{4+} ions are rather small in size and their volume fraction is much less than that of the semiconducting matrix. For this reason, apparently, the transition of these isolated clusters to more conductive FM state with temperature decreasing does not show itself either in $I(T)$ [Fig. 10(a)] or in $\rho(T)$ (Fig. 4) dependences. The TKE value characterizing the FM contribution is, however, quite high { only three times less than that for $x = 0.35$. TKE has a maximum at 118 K. After cooling in zero field, another feature (a shoulder) appears at $T' = 60$ K [Fig. 1(a)]. A maximum at nearly the same temperature $T_g = 60\{70$ K was found earlier in temperature dependences of the AC and DC susceptibility for bulk $\text{La}_{0.85}\text{Sr}_{0.15}\text{CoO}_3$ [9, 10, 12, 13] and attributed to spin-glass freezing. Magnetization temperature curves for $\text{La}_{0.85}\text{Sr}_{0.15}\text{CoO}_3$ show a cusp at the same freezing temperature T_g [11, 30]. It can be thought that the above-mentioned feature in the TKE temperature curve near the temperature $T = 60$ K [Fig. 1(a)] is determined by the same effect.

It should be noted that the highest MR and its anisotropy for this film are observed in the range 60{80 K [Fig. 6(c)]. The ratio of MRs measured in fields parallel and perpendicular to the film plane is close to 2. At $T = 4.2$ K and 20.4 K the values of field H_p are found to be rather high ($H_{pk} = 7.0$ kOe and $H_{p?} = 4.5$ kOe for field orientation parallel and perpendicular to the film plane, respectively). At $T = 78$ K and above the MR hysteresis is practically unobservable. Taking into account that field H_p is equal to the coercive force H_c (see Sec. IIIB above) this behavior is quite consistent with the assumed cluster-glass state at this doping level. A cluster glass is actually a system of small FM (single domain) particles. An isolated particle should have enough thermal energy to surmount the energy

barrier $E = KV$ (K is the anisotropy constant, V is the particle volume) to reverse its magnetization in magnetic field [31, 32]. For a system of such particles there is the so called blocking temperature, T_B , below which the particle moment is blocked. The mean blocking temperature, $\langle T_B \rangle / K_m V_m$, is determined by mean values (K_m and V_m) of the anisotropy constant and particle volume [31]. The above-mentioned temperature T_g is directly related to $\langle T_B \rangle$ by relation $T_g = \langle T_B \rangle$ [31], where α is a numerical factor of the order of unity depending on the form of the particle size distribution. The higher is temperature, the smaller is H_c . According to Ref. [32], $H_c \propto (1 - T/T_B)^{1/2}$, so that at $T > \langle T_B \rangle$ the system becomes superparamagnetic. It is therefore most probable that the linear magnetic-field dependence of TKE in this film at $T = 91$ K (near Kerr effect maximum) (Fig. 3) is determined by the superparamagnetic behavior of the clusters. The high H_p field for the film with $x = 0.15$ agrees with the H_c data obtained on a bulk polycrystal of the same composition [30].

The FM interaction in clusters is mainly attributable to the Co^{3+} (IS)-O- Co^{4+} (LS) superexchange or the double-exchange of localized t_{2g} electrons via itinerant e_g electrons [9]. As another source of FM state, the magnetic polarons formed near the Co^{4+} ions can be mentioned [22]. The hole-rich regions stabilize IS state of Co^{3+} ions at the interface to the hole-poor regions. The clusters are thought to be coupled antiferromagnetically (AFM) through the superexchange interaction between the Co^{3+} (IS) ions [9]. Since the clusters are distributed randomly, the intercluster exchange is frustrated and the cluster moments have non-collinear orientation. This leads to a large anisotropy below the temperature T_g . The influence of all these factors on magnetic properties can show itself as a typical spin-glass-like behavior.

Among the films studied, this film has the highest MR [Fig. 6(c)]. It is difficult to imagine that strengthening of the magnetic order in small isolated clusters embedded in a semiconducting matrix, can cause this rather strong effect [19]. It should be suggested, therefore, that an applied magnetic field enhances the intercluster tunneling and/or increases the conductivity of intercluster semiconducting regions. It is quite probable that magnetic field affects somehow the interface regions between hole-rich clusters and hole-poor matrix (which are enriched with Co^{3+} ions in IS state [9]). It was argued in Ref. [10] that the volume of the superparamagnetic clusters should increase in a magnetic field, that can cause a considerable MR effect. These suggestions need, however, an elaboration and verification in a further study.

2. $La_{0.75}Sr_{0.25}CoO_3$ film

When the Sr concentration is raised to $x = 0.25$, the content of holes in clusters increases. The volume of the FM clusters increases too and the exchange in them is enhanced by charge carriers (double exchange). A decrease in transmittance with temperature decreasing on cooling below the temperature of the metal-insulator transition $T_{MI} \approx 180$ K [Fig. 10(a)] together with no signs of the transition to metallic state at this temperature in $\rho(T)$ dependence (Fig. 4) indicates that in the film with $x = 0.25$ the transition to FM metallic state near 180 K occurs only in the isolated hole-rich clusters (embedded in a semiconducting matrix) rather than in the whole volume of the film. For this reason there are no continuous metallic conducting paths penetrating the whole film and, therefore, the transition of the clusters to the FM state has no visible effect on recorded $\rho(T)$ behavior (Fig. 4). But this transition is reflected in the MR temperature behavior which is shown in Fig. 6(b).

It can be seen that the MR reaches its maximum below $T \approx 200$ K which agrees well with the magneto-optical and optical data obtained [see Figs. 1(b) and 10(a)]. Generally, the temperature behavior of MR for this Im corresponds to that of highly inhomogeneous magnetic system, as it was mentioned already in Sec. IIIB.

No significant MR anisotropy or MR hysteresis has been found in this Im . It is caused, perhaps, by proximity of composition to the percolation threshold ($x_c = 0.20\{0.25\}$), near which cluster sizes and orientations are most chaotic. TKE appears at $T \approx 230$ K, i.e. above the temperature $T_{MI} \approx 180$ K obtained from the transmittance data. The relation $T_{MI} < T_c$ is expected for this range of Sr doping [10]. The field dependence of the TKE (Fig. 3) exhibits a typical FM behavior at the temperature ($T \approx 180$ K), where the TKE is maximum, but it is linear at $T = 70$ K, which is typical of superparamagnetic system, but can also be determined by a change in the relationship between the FM and AFM contributions responsible for magnetism of this Im with lowering temperature.

3. $\text{La}_{0.65}\text{Sr}_{0.35}\text{CoO}_3$ Im

For $x > x_c$, the volume fraction of hole-rich regions should be high enough to form an infinite percolating FM cluster below T_c [9]. The results for the Im with $x = 0.35$ support well this view. Both, the $\rho(T)$ and $I(T)$ dependences [Figs. 5 and 10(a)] manifest that the metal-insulator transition starts at $T \approx 250$ K. The temperature behavior of the MR is typical of optimally doped cobaltites, with a sharp maximum at $T = 230$ K which corresponds to the Curie temperature for this Im . At that, the metallic behavior of $I(T)$ is more pronounced than for $x = 0.25$, but a strong anomaly can be seen in the range 160–220 K. The maximum Kerr effect is found to be larger for $x = 0.35$ than that of for $x = 0.25$, and the temperature range of maximal Kerr effect magnitude is wider [Fig. 1(c)]. At the same time the magnitude of Kerr effect drops sharply below 160 K. The same as for $x = 0.25$, the field dependence of TKE (Fig. 3) exhibits a typical FM behavior for the temperature range, where $\rho(T)$ is maximum, but it is linear at $T = 96$ K.

Although at $x = 0.35$ the infinite FM cluster, percolating through the whole sample, is formed, at the same time, however, a pervasive hole-poor matrix with some isolated clusters in it persists up to $x = 0.5$ [9]. The large cluster interfaces and/or the interlayer between the FM grains contain Co^{3+} (IS) ions which change into the LS state with lowering temperature and no longer assist the charge transport and Kerr effect. As the number of Co^{3+} (IS) ions reduces and the related FM interaction grows weaker, the carriers can gradually localize in the FM clusters themselves. This mechanism is maybe responsible for the rather high resistivity of the Im with $x = 0.35$ below $T = 50$ K and for the hysteretic and anisotropic behavior of MR. The low-temperature resistance minimum is typical of polycrystalline samples with weak enough interconnections between FM grains. In this case the intergrain tunneling can become activated at low enough temperature that leads to non-metallic behavior of $\rho(T)$ [19]. It is clear that magnetical inhomogeneity due to the phase separation can contribute to this effect in the same way as polycrystalline structure. The MR hysteresis is found to be absent above 90 K, but fields H_p are significant already at $T = 78$ K ($H_{pk} = 2.5$ kOe and $H_{p?} = 2.0$ kOe). With temperature decreasing down to $T = 42$ K the H_p values have increased up to $H_{pk} = 4.5$ kOe and $H_{p?} = 5.3$ kOe. The strong decrease in TKE and change in character of field dependence of it for decreasing temperature, together with rather high MR anisotropy and the considerable growth of H_p in low temperature range, indicate that in spite of metallic behavior of the Im conductivity,

FM state in it is not homogeneous and maybe close to cluster-glass state.

C. Transmittance anomaly and orbital ordering of Co^{3+} (IS) ions.

The features of the temperature and spectral behavior of optical and magneto-optical properties, considered above, can be determined by the transition of Co^{3+} ions from LS state to either or both HS and IS states. In the transmittance spectra, however, the special anomaly is found, which can be attributed only to the LS-IS transition. This anomaly in the $I(T)$ dependence (kinked behavior of it) is observed for all LaCoO_3 samples studied and appears practically in the same temperature range 160–220 K [Fig. 10 (a)]. It can be seen quite clearly for the samples with $x = 0.15$ and $x = 0.35$ on the background of the general semiconductive or metallic run of their $I(T)$ curves. For the sample with $x = 0.25$ the temperature range of the anomaly nearly coincides with the temperature T_{MI} and, therefore, the anomaly is not so distinct. The anomaly of this type is never mentioned for manganites. It is reasonable, therefore, to assume that its nature is determined by some specific feature of cobaltites. This is the transition of Co^{3+} ions from LS state to a higher-spin state with increasing temperature. According to the Ising model molecular-field calculations, an energy gap, $\Delta = 230$ K, between the $S = 0$ and $S = 1$ spin states provides a good description for the temperature dependence of magnetic susceptibility [26]. The spin transition proceeds gradually. No information can be found in literature about special temperature points of this transition, except for the Mossbauer effect in LaCoO_3 [33]. The latter data permit the conclusion that the ratio between the Co^{3+} (HS) concentration and the total Co^{3+} content reaches its maximum at $T \approx 200$ K. It follows, however, from neutron scattering data for LaCoO_3 [10] that the 50:50 ratio of low-spin and higher-spin Co^{3+} ions is stable in a wide interval from 110 K to room temperature, which is supported by the results for magnetic susceptibility [34].

According to electron structure calculation for LaCoO_3 [3], with rising temperature the LS ($S = 0$) state of Co ions transfer to the IS ($S = 1$) state rather than to HS ($S = 2$) one. Energetically, the latter state appears to be higher than the IS state even above $T \approx 600$ K. The Co^{3+} (IS) ion with the $(t_{2g}^5 e_g^1)$ configuration is a Jahn-Teller (JT) ion. In the case of equal spins, the orbitally ordered (non-metallic) state is more preferable than the state without orbital order [3]. In this case the non-metallic behavior of LaCoO_3 at $90 \text{ K} < T < 500 \text{ K}$ can be described properly assuming that Co^{3+} ions are in the orbital-ordered state. The gradual transition to the metallic behavior observed experimentally at $T > 550 \text{ K}$ is associated with the destroying the orbital order [3]. The presence of JT Co^{3+} (IS) ions in cobaltites is supported by experimental results, such as anomalous splitting of phonon modes in LaCoO_3 [6] and giant anisotropic magnetostriction in $\text{La}_{1-x}\text{Sr}_x\text{CoO}_3$ [35]. Measurement of magnetic circular dichroism spectra has revealed the presence of Co^{3+} (IS) ions with a finite orbital moment [36].

It is possible that the $I(T)$ anomaly appears because the orbital-ordered Co^{3+} (IS) ions reach their maximum concentration at $T \approx 180 \text{ K}$. At $T > 180 \text{ K}$ the ions transfer gradually into the orbital-disordered state. The anomalous splitting of phonon modes in the spectrum of LaCoO_3 [6] strengthens this hypothesis. The mode corresponding to the orbital-ordered state becomes saturated at $T \approx 200 \text{ K}$ whereas the intensity of the mode ascribed to the orbital-disordered state increases sharply above $T \approx 160 \text{ K}$.

As the LS-IS transition occurs in some fraction of the Co ions, two features are expected in the optical spectra of mixed-valence cobaltites: (i) appearance of new absorption lines

corresponding to the optical transitions including energy states of Co^{2+} (IS) ions and (ii) charge-carrier localization caused by JT lattice distortions near Co^{3+} (IS) ions, which may entail the formation of JT polarons. The intricate $I(T)$ dependence near the absorption edge (1.0{1.4 eV} [Fig. 10 (b)] is determined, probably, by the appearance of additional absorption bands, which, however, are not resolved in this spectral range. These bands can have different temperature dependence, including the anomalous ones, and their superposition would result in tangled appearance of $I(T)$ dependence.

A possible reason for the $I(T)$ anomaly in the region of light interaction with the charge carriers at $E = 0.20$ eV [Fig. 10 (a)] can be charge localization at the maximum concentration of the orbital-ordered JT Co^{3+} (IS) ions. It is natural to assume that the orbital-ordered Co^{3+} (IS) ions reside in the hole-poor matrix (for $x = 0.15$ and 0.25) or in the regions near the boundaries of hole-rich clusters (for $x = 0.35$). The hole-rich clusters are expected to contain orbital-disordered Co^{3+} (IS) ions. The $I(T)$ anomaly can appear only when contributions of these two mechanisms { enhancing of metallic behavior of charge carriers in the clusters and localization of charge carriers in the matrix } are comparable. It should be noted that this mechanism of charge-carrier localization is possible only for JT ions in semiconducting matrix, that is for Co^{2+} (IS) ions. There is no such mechanism for LS-HS transition of Co^{3+} ions. Cooling in a finite applied field, or cooling at $H = 0$ and subsequent measurement at $H > 0$, suppresses the anomaly in $I(T)$, i.e. enhances the metallic contribution of the charge carriers [see Fig. 10 (c) for $x = 0.35$]. The anomaly is affected most significantly by fast cooling of the sample preheated to $T = 320$ K [Fig. 10 (c)]. At this temperature the significant fraction of Co^{3+} (IS) ions in the semiconducting matrix becomes orbital-disordered. On fast cooling this "disordered" (and more metallic) state is frozen. After such thermal treatment the $I(T)$ anomaly vanishes completely both at $E = 0.20$ eV (Fig. 10) and at $E = 1.0$ eV (not shown). The metallic contribution becomes more pronounced as well. Appearance and change in number of orbital-ordered Co^{3+} (IS) ions in dielectric matrix can be responsible for unusual behavior of TKE temperature dependence for films with $x = 0.25$ as well.

At $T = 80$ K, Kerr effect is equally small in the film with $x = 0.25$ and $x = 0.35$, and it is smaller than in the film with $x = 0.15$ (Fig. 1). This is because only a small fraction of Co^{3+} (IS) ions are involved in the FM exchange at 70{90 K. In film with $x = 0.25$, Co^{3+} (IS) ions are fewer than in the film with $x = 0.15$ if we assume that the highest Co^{3+} (IS) concentration is 50% of all Co^{3+} ions both in non-doped LaCoO_3 and doped $\text{La}_{1-x}\text{Sr}_x\text{CoO}_3$. Besides, it is likely that in the matrix and in the boundary regions of metallic clusters the Co^{3+} (IS) ions are in the orbital-ordered state, so they interact antiferromagnetically. As a result, the number of the ions involved in the FM interaction is much less than 50% of the total Co^{3+} content corresponding to the nominal film composition. The linear behavior of TKE as a function of magnetic field which is observed in all the films below the TKE peak (Fig. 3) shows that the FM interaction (double exchange) weakens, and concurrence the FM interaction (in clusters) and AFM interaction (in the matrix or boundary regions) comes into play.

An unusual fact is observed for the film with $x = 0.35$: on heating in a weak field ($H = 0.9$ kOe), the TKE dependence shifts significantly towards higher temperature when compared with that of at $H = 3.5$ kOe [Fig. 1 (c)]. This finding implies that when Kerr effect is measured in the magnetic field 3.5 kOe, the Co^{3+} (LS)- Co^{3+} (IS) transition is driven not only by temperature but by the magnetic field as well. The spin transition should actually occur at higher temperatures, and the magnetic field stimulates its onset at lower temperatures. This conclusion was arrived in Ref. 35 at explaining the giant anisotropic

magnetostriction of $\text{La}_{1-x}\text{Sr}_x\text{CoO}_3$ ($x = 0.3$). The curves obtained for the film with $x = 0.35$ are shifted after heating-cooling in a strong field [Fig. 3 (c)] because heating stimulates an earlier onset of the LS-IS transition and cooling "freezes" the state which existed at the high temperature. The temperature hysteresis of TKE is small at $x = 0.25$ presumably because the onset of FM and metal-insulator transition in clusters takes place within the interval $T = 180\text{--}200\text{ K}$, where the content of orbital-ordered JT ions and, hence, the related AFM contribution are the highest. The state without orbital order has a larger magnetic moment [3], which orders a strong TKE even above the temperature of metal-insulator transition. The considerable TKE shift towards higher temperatures caused by fast cooling of the film with $x = 0.25$ [Fig. 1 (b)] agrees well with the effect produced by fast cooling on the $I(T)$ curves [Fig. 10 (c)]. The fast cooling of the film which is partially in the orbital-disordered state (at $T = 300\text{ K}$) is favorable for "freezing" this state. As a result, the carrier localization weakens, the AFM component decreases and the FM contribution increases.

The evolution of optical, magneto-optical and transport properties of the films studied with the doping level correlates well with the concept of electron phase separation in cobaltites. At a low doping level ($x = 0.15$), the Co^{3+} (LS)- Co^{3+} (IS) transition in the magnetic field begins at helium temperatures. The transition enhances the FM contribution in the clusters, which is mainly connected with the Co^{3+} (IS) - O^{2-} - Co^{4+} (LS) superexchange. As a result, the Kerr effect grows up to $T = 118\text{ K}$. On the further rise of temperature the number of Co^{3+} (IS) ions increases. The content of orbital-ordered ions in the matrix increases too and so does the related AFM contribution. In the temperature region, where the content of the orbital-ordered Co^{3+} (IS) ions is the highest ($T \approx 180\text{ K}$), the AFM contribution exceeds the FM one from the clusters and the Kerr effect turns to zero. The high coercive forces are indicative of small sizes of the FM clusters in the non-magnetic matrix. The magnetic state of the film with $x = 0.15$ has doubtless features of the spin-glass state.

On doping level ($x = 0.25$) near the percolation threshold, the hole-rich FM clusters are quite numerous, but segregated. No infinite cluster is formed yet. In the clusters the metal-insulator transition occurs near 180 K . This suggests that below 180 K the FM interaction is mainly connected with the charge carrier exchange (double exchange). Because of doping, the total content of Co^{3+} ions is smaller than at $x = 0.15$ and the Kerr effect is also smaller at low temperatures. It is likely that the fraction of the orbital-ordered Co^{3+} (IS) ions grows with temperature only in the matrix and becomes the highest at $T \approx 180\text{ K}$. Since the degree of orbital ordering decreases above this temperature, TKE remains appreciably strong up to $T = 230\text{ K}$ because the state without orbital ordering has a large moment.

At the doping level ($x = 0.35$) above the percolation threshold, the FM regions percolate magnetically as well as conductively through the whole film. For this reason the temperature of metal-insulator transition is close to $T_c = 230\text{ K}$. Although the number of Co^{3+} ions involved in the LS-IS transition decreased, the TKE maximum is much higher than at $x = 0.25$ because the double exchange assisted by Co^{4+} ions enhances the FM contribution. The film is, however, magnetically inhomogeneous, which is evident from the TKE hysteresis under the heating-cooling condition. The considerable hysteresis and the strong dependence of TKE on the sample prehistory and thermal treatment may be connected with orbital ordering in the cluster interfaces, which are the sources of the AFM contribution. As in the $x = 0.25$ case, the FM state of the film with $x = 0.35$ below the temperature of TKE maximum becomes much weaker due to the enhanced AFM interaction. This is evident from the sharp growth of H_c with decreasing temperature typical of the cluster glass state.

V. CONCLUSION

Optical, magneto-optical and transport properties of polycrystalline $\text{La}_{1-x}\text{Sr}_x\text{CoO}_3$ ($x = 0.15; 0.25; 0.35$) films have been studied. Unlike manganites, no direct correlation is found between the temperature of metal-insulator transition in clusters and the temperature at which the FM contribution appears. It is found that the temperature dependences of the optical and magneto-optical properties of the films exhibit features, which can be determined by the transition of Co^{3+} ions from the low-spin state ($S = 0$) to the intermediate spin state $S = 1$. This transition is driven not only by temperature increase but by an applied magnetic field as well. It is shown as well that the above-indicated properties are dependent on the number of orbital-ordered Co^{3+} ions in semiconducting matrix. Irrespective of the Sr concentration, the content of the orbital-ordered Co^{3+} ions is the highest at $T \approx 180$ K. The results obtained support the phase separation scenario for mixed-valence cobaltites.

Acknowledgments

The authors thank M. A. Korotin for helpful discussions. The study is partially supported by RFBR Grants No. 02-02-16429 and No. 00-02-17797.

-
- [1] R. von Helmolt, J. Wecker, B. Holzapfel, L. Schultz, and K. Samwer, Phys. Rev. Lett. 71, 2331 (1993); S. Jin, T. H. Tie, M. M. McCormack, R. A. Fastnacht, R. Ramesh, and L. H. Chen, Science 264, 413 (1994).
 - [2] P. M. Raccach and J. B. Goodenough, Phys. Rev. B 155, 932 (1967).
 - [3] M. A. Korotin, S. Yu. Ezhov, I. V. Solovyev, V. I. Anisimov, D. I. Khomskii, and G. A. Sawatzky, Phys. Rev. B 54, 5309 (1996).
 - [4] P. Ravindran, H. Fjellvåg, A. Kjekshus, P. Blaha, K. Schwarz, and J. Luitz, J. Appl. Phys. 91, 291 (2002).
 - [5] T. Saitoh, T. Mizokawa, A. Fujimori, M. Abbate, Y. Takeda, and M. Takano, Phys. Rev. B 56, 1290 (1997).
 - [6] S. Yamaguchi, Y. Okimoto, and Y. Tokura, Phys. Rev. B 55, R8666 (1997).
 - [7] Y. Kobayashi, N. Fujiwara, S. Murata, K. Asai, and H. Yasuoka, Phys. Rev. B 62, 410 (2000).
 - [8] C. Zobel, M. Kriener, D. Bruns, J. Baier, M. Grüniger, T. Lorenz, P. Reutler, and A. Revcolevschi, Phys. Rev. B 66, 020402 (R) (2002).
 - [9] M. A. Senaris-Rodriguez and J. B. Goodenough, J. Sol. State Chem. 118, 323 (1995).
 - [10] R. Caciuo, D. Rinaldi, G. Barucca, J. Mira, J. Rivas, M. A. Senaris-Rodriguez, P. G. Radaelli, D. Fiorani, and J. B. Goodenough, Phys. Rev. B 59, 1068 (1999).
 - [11] M. Itoh, I. Natori, S. Kubota, and K. Motoya, J. Phys. Soc. Jap. 63, 1486 (1994).
 - [12] P. S. Anil Kumar, P. A. Joy, and S. K. Date, J. Appl. Phys. 83, 7375 (1998).
 - [13] J. Mira, J. Rivas, G. Bab, G. Barucca, R. Caciuo, D. Rinaldi, D. Fiorani, and M. A. Senaris-Rodriguez, J. Appl. Phys. 89, 5606 (2001).
 - [14] N. N. Loshkareva, Yu. P. Sukhorukov, E. A. Gan'shina, E. V. Mostovshchikova, R. Yu. Kumeritova, A. S. Moskvina, Yu. D. Panov, O. Yu. Gorbenko, and A. R. Kaul, JETP 92, 462 (2001).

- [15] N. N. Loshkareva, Yu. P. Sukhorukov, E. V. Mostovshchikova, E. V. Nomerovannaya, A. A. Makhnev, S. V. Naumov, E. A. Gan'shina, I. K. Rodin, A. S. Moskvina, and A. M. Balbashev, *JETP* 94, 350 (2002).
- [16] J. Schoenes "Magnetooptical Properties of Metals, Alloys and Compounds", in *Materials Science and Technology*, edited by R. W. Cahn, P. Haasen and E. J. Kramer, Vol. 3, *Electronic and Magnetic Properties of Metals and Ceramics*, Vol. Editor K. H. J. Buschow (1990).
- [17] A. K. Zvezdin and V. A. Kotov, "Modern Magnetooptics and Magnetooptical Materials" (IOP Publishing LTD, Bristol, 1997).
- [18] E. A. Balykina, E. A. Gan'shina, and G. S. Krinichik, *Zh. Exp. Teor. Fiz.* 93, 1879 (1987).
- [19] B. I. Belevtsev, N. T. Cherpak, I. N. Chukanova, A. I. Gubin, V. B. Krasovitsky, and A. A. Lavrinovich, *J. Phys.: Condens. Matter* 14, 2591 (2002).
- [20] B. I. Belevtsev, V. B. Krasovitsky, A. S. Pan'kov, and I. N. Chukanova, Preprint cond-mat/0207346.
- [21] M. Ziese, *Rep. Prog. Phys.* 65, 143 (2002).
- [22] S. Yamaguchi, Y. Okimoto, H. Taniguchi, and Y. Tokura, *Phys. Rev. B* 53, R2926 (1996).
- [23] N. N. Loshkareva, N. I. Solin, Yu. P. Sukhorukov, N. I. Lobachevskaya, and E. V. Pan'lova, *Physica B* 293, 390 (2001).
- [24] Yu. P. Sukhorukov, N. N. Loshkareva, E. A. Gan'shina, A. R. Kaul, O. Yu. Gorbenko, and K. A. Fatieva, *Techn. Phys. Lett.* 25, 551 (1999); Yu. P. Sukhorukov, E. A. Gan'shina, B. I. Belevtsev, N. N. Loshkareva, A. N. Vinogradov, K. D. D. Rathnayaka, A. Parasiris, and D. G. Naugle, *J. Appl. Phys.* 91, 4403 (2002).
- [25] T. Arima, Y. Tokura, and J. B. Torrance, *Phys. Rev. B* 48, 17006 (1993).
- [26] Y. Tokura, Y. Okimoto, S. Yamaguchi, H. Taniguchi, T. Kimura, and H. Takagi, *Phys. Rev. B* 58, R1699 (1998).
- [27] S. Yamaguchi, Y. Okimoto, K. Ishibashi, and Y. Tokura, *Phys. Rev. B* 58, 6862 (1998).
- [28] I. Solovyev, N. Hamada, and K. Terakura, *Phys. Rev. B* 53, 7158 (1996).
- [29] A. S. Moskvina, E. V. Zenkov, Yu. D. Panov, N. N. Loshkareva, Yu. P. Sukhorukov, and E. V. Mostovshchikova, *Fiz. Tverd. Tela* 44, 1452 (2002).
- [30] V. Golovanov, L. Mihaly, and A. R. Moodenbaugh, *Phys. Rev. B* 53, 8207 (1996).
- [31] R. W. Chantrell, M. El-Hilo, and K. O'Grady, *IEEE Trans. Magn.* 27, 3570 (1991).
- [32] P. Katiyar, D. Kumar, T. K. Nath, A. V. Kvit, J. Narayan, S. Chattopadhyay, W. M. Gilmore, S. Coleman, C. B. Lee, J. Sankar, and Rajiv K. Singh, *Appl. Phys. Lett.* 79, 1327 (2001).
- [33] V. G. Bhidre, D. S. Rajpuri, G. R. Rao, and C. N. R. Rao, *Phys. Rev. B* 6, 1021 (1972).
- [34] M. A. Senaris-Rodriguez and J. B. Goodenough, *J. Sol. State Chem.* 116, 224 (1995).
- [35] M. R. Ibarra, R. Mahendiran, C. Marquina, B. Garcia-Landa, and J. Blasco, *Phys. Rev. B* 57, R3217 (1998).
- [36] K. Yoshi, M. Mizumaki, Y. Saitoh, and A. Nakamura, *J. Sol. State Chem.* 152, 577 (2000).

Figure captions

Figure 1. Temperature dependences of TKE of $\text{La}_{1-x}\text{Sr}_x\text{CoO}_3$ films with $x = 0.15$ (a), $x = 0.25$ (b) and $x = 0.35$ (c). Heating and cooling regimes are indicated by arrows. All curves were recorded in magnetic field $H = 3.5$ kOe at photon energy $E = 2.8$ eV, except dashed-line curve for $x = 0.35$, which was recorded on heating in field $H = 0.9$ kOe. Solid line in the picture for $x = 0.25$ (b) corresponds to fast cooling. Rates of heating and cooling were usually in the range $1\text{--}3$ K/min, the "fast cooling" was done with a rate about 20 K/min.

Figure 2. Spectral dependences of TKE of the $\text{La}_{1-x}\text{Sr}_x\text{CoO}_3$ films at temperatures of maximum in the temperature dependence of TKE.

Figure 3. Magnetic-field dependences of TKE of the $\text{La}_{1-x}\text{Sr}_x\text{CoO}_3$ films studied at temperatures, corresponding to the maximal TKE effect (190 K for $x = 0.35$ and 180 K for $x = 0.25$), and at much lower temperatures.

Figure 4. Temperature dependences of the resistivity of the films $\text{La}_{1-x}\text{Sr}_x\text{CoO}_3$ (in semilogarithmic coordinates).

Figure 5. Temperature dependence of the resistivity of film $\text{La}_{0.65}\text{Sr}_{0.35}\text{CoO}_3$.

Figure 6. Temperature dependences of magnetoresistance $[R(H) - R(0)]/R(0) = R(H)/R(0)$ at $H = 20$ kOe of the $\text{La}_{1-x}\text{Sr}_x\text{CoO}_3$ films. The fields H_k and H_\perp were applied parallel and perpendicular to the film plane, respectively. In both cases the fields were perpendicular to the transport current. The MR of the film with $x = 0.25$ (b) has not shown a noticeable sensitivity to the angle between the field and the film plane.

Figure 7. Magnetoresistive hysteresis for $\text{La}_{1-x}\text{Sr}_x\text{CoO}_3$ film with $x = 0.35$ at $T = 78$ K. Applied fields were parallel (H_k) and perpendicular (H_\perp) to the film plane. In both cases the fields were perpendicular to the transport current.

Figure 8. Optical density spectra $D = \ln(I_0/I)$ (I_0 is the incident-light intensity, I is the intensity of light transmitted through the film) for $\text{La}_{1-x}\text{Sr}_x\text{CoO}_3$ films studied in the visible light range at $T = 295$ K. The curves are spaced apart for facilitation of visual perception.

Figure 9. Optical density spectra $D = \ln(I_0/I)$ (I_0 is the incident-light intensity, I is the intensity of light transmitted through the film) for $\text{La}_{1-x}\text{Sr}_x\text{CoO}_3$ films studied in the IR range at different temperatures.

Figure 10. Temperature dependences of the intensity of light transmitted through the $\text{La}_{1-x}\text{Sr}_x\text{CoO}_3$ films at $E = 0.20$ eV (a), in the energy range $1.0\text{--}1.4$ eV (b) and for different measurement conditions at $E = 0.20$ eV for film with $x = 0.35$ (c). The numerals in panel (c) of the figure indicate the following: 1 { ZFC, $H = 0$; 2 { FC, $H = 0$; 3 { ZFC, $H = 8$ kOe; 4 { fast cooling after a heating up to $T = 320$ K, $H = 0$ (heating with the rate about $1\text{--}1.5$ K/min; the following "fast cooling" from 320 K to $T = 80$ K have taken about 10 min). The curves in panels (a) and (b) are spaced apart for facilitation of visual perception.

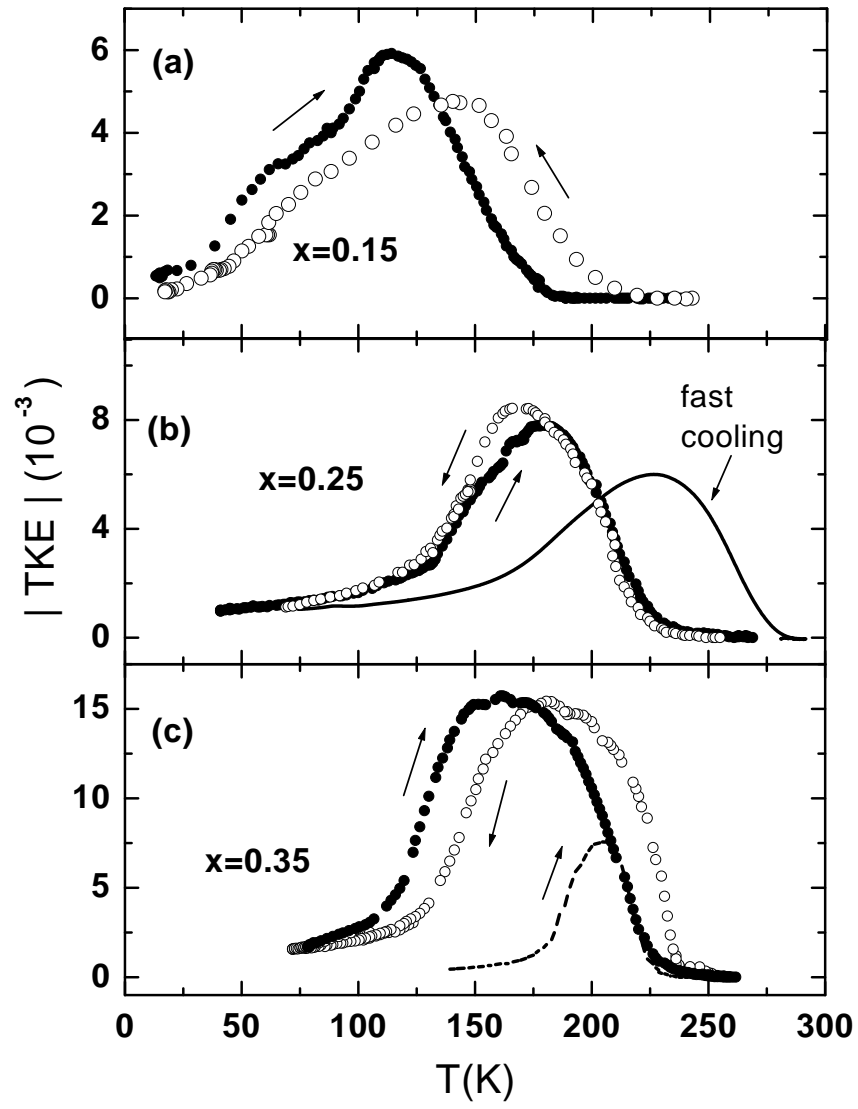


Figure 1 to paper Loshkareva et al. (Phys. Rev. B)

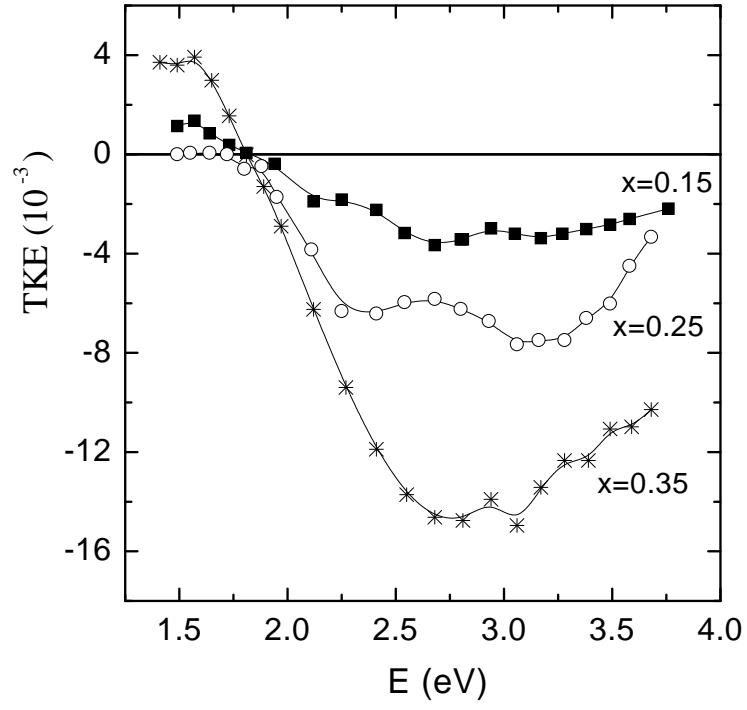


Figure 2 to paper Loshkareva et al. (Phys. Rev. B)

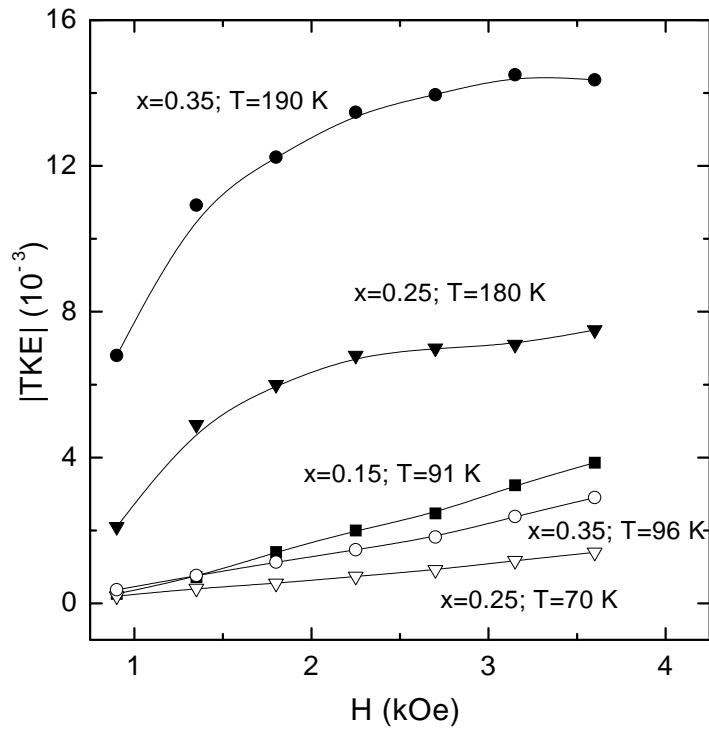


Figure 3 to paper Loshkareva et al. (Phys. Rev. B)

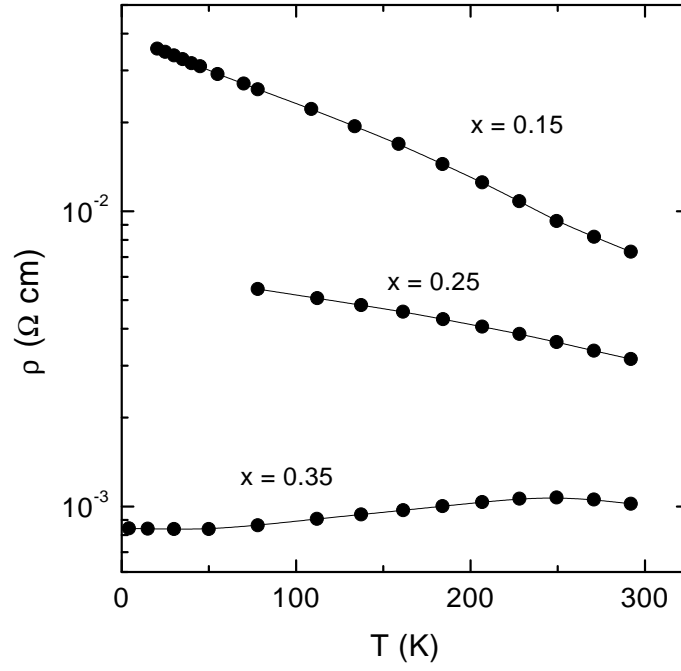


Figure 4 to paper Loshkareva et al. (Phys. Rev. B)

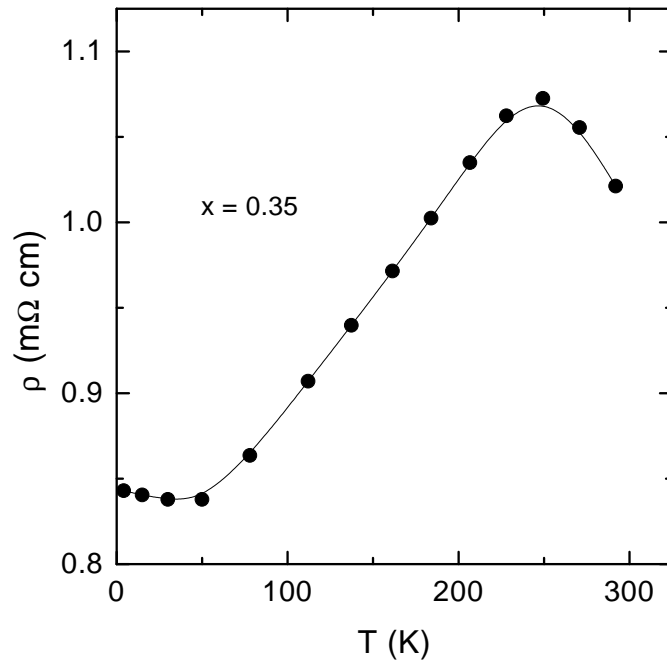


Figure 5 to paper Loshkareva et al. (Phys. Rev. B)

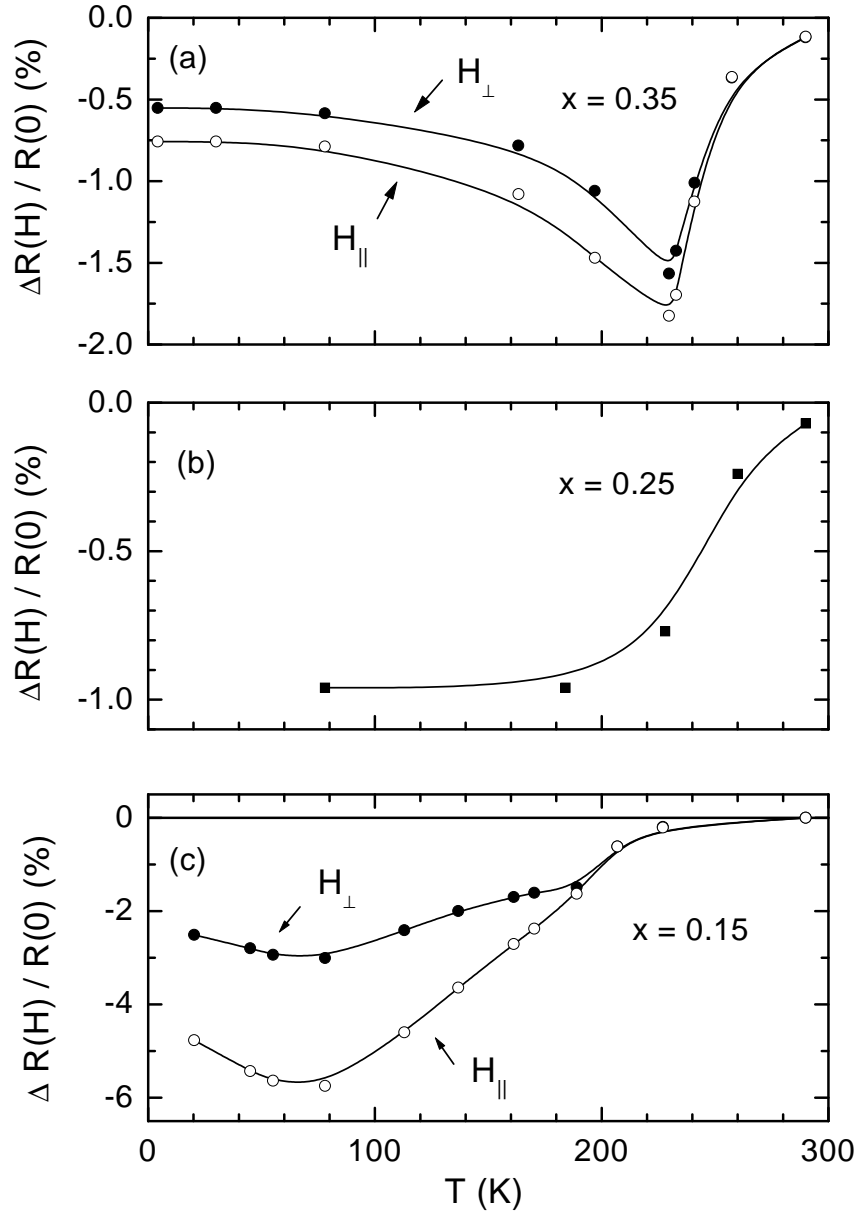


Figure 6 to paper Loshkareva et al. (Phys. Rev. B)

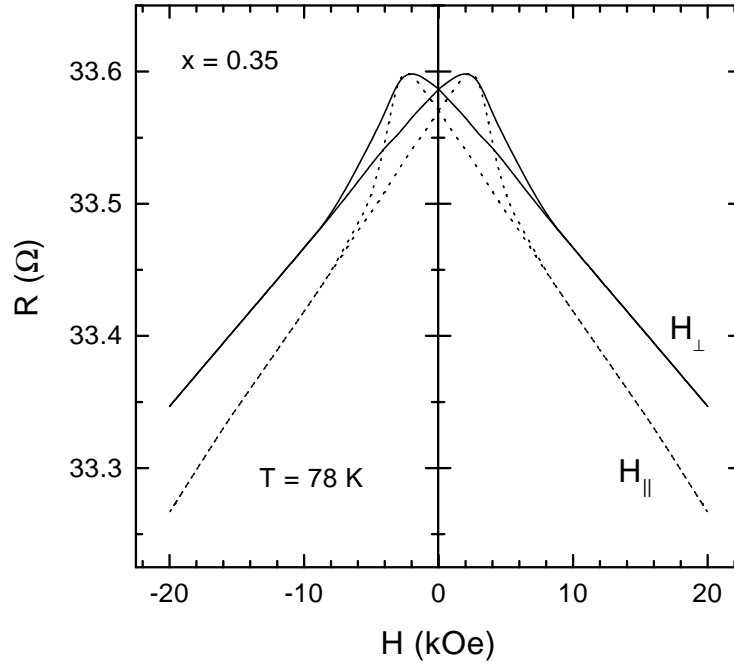


Figure 7 to paper Loshkareva et al. (Phys. Rev. B)

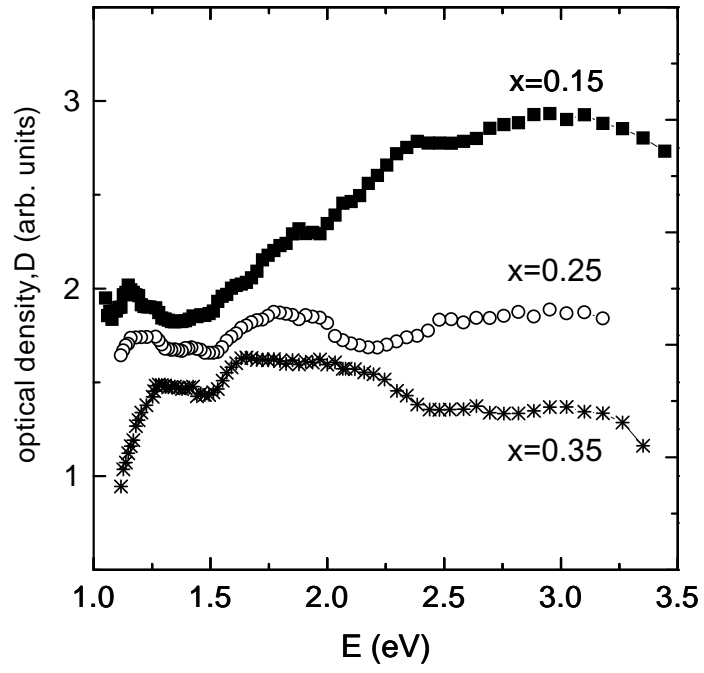


Figure 8 to paper Loshkareva et al. (Phys. Rev. B)

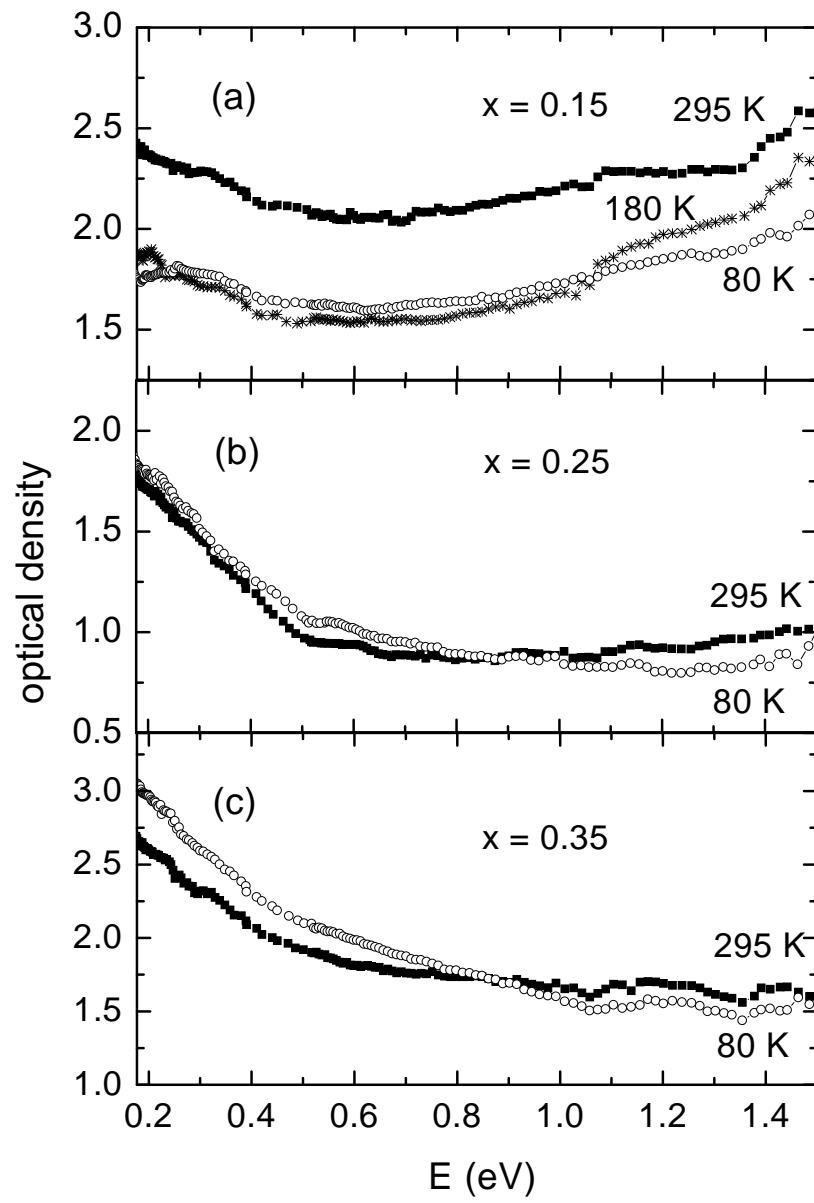


Figure 9 to paper Loshkareva et al.

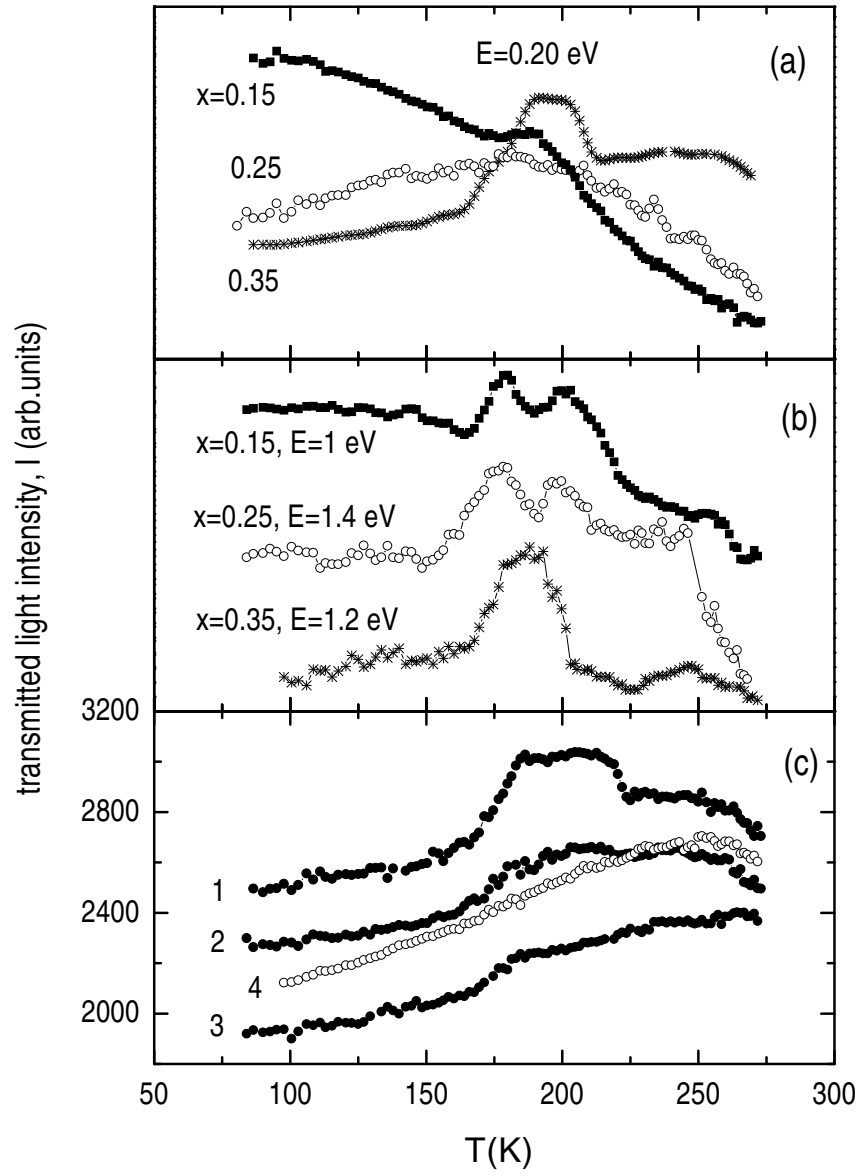


Figure 10 to paper Loshkareva et al.